

Where Crystal Planes Meet: Contribution to the Understanding of the Tin Whisker Growth Process

André Egli, Wan Zhang, Jochen Heber, Felix Schwager
ShipleY Schweiz AG
Littau-Lucerne, Switzerland

Michael Toben
ShipleY Company, LLC
Freeport, NY

Abstract

The texture of a tin deposit has been described as a key factor influencing whisker growth. Based on X-ray diffraction (XRD) and whisker growth data, this paper intends to show one possible mechanism that contributes to the formation of whiskers. By correlating observed XRD patterns with whisker growth performance in tin electrodeposits, a model has been created to approximate the risk of whisker growth. With some limitations, this model was found to be valid in predicting the extent of whisker growth in tin deposits.

Introduction

During the last twenty years, it has been periodically reported that crystallographic characteristics of tin deposits contribute to whisker growth. Lee and Lee for example showed that whiskers mainly grow from grains having a different crystal orientation than the main texture.¹ Zhang et al. correlated crystal orientations with morphology and whisker density.²

In this publication, the finding of a correlation *between* the crystal planes within the tin electrodeposit is presented, which provides a possible explanation for the influence of the crystallographic texture of a tin deposit on its propensity to grow whiskers. Furthermore, this finding is used to develop an empirical model to approximate the risk of an electrodeposit to grow whiskers.

Observation of ‘High-Risk’ Crystal Planes

Our own interest in XRD was aroused during the development of lead-free tin deposition processes, when it was observed that deposits with a higher abundance of certain crystal planes were more prone to whisker growth than others lacking those particular crystal planes in a Θ - 2Θ scan. Those particular crystal planes were (103), (321), and (420) and the question emerged as to what these planes have in common.

Interplanar Angles

The only common feature that has been identified is that these ‘high-risk’ planes (or peaks as seen by XRD) always appeared in a very distinct pattern of peaks. For example, the (103) peak is very often accompanied by the (101) peak; the (321) by the (211); and the (420) by the (220). Frequently, the accompanying peaks correspond to the main texture of the deposit, which is in agreement with Lee and Lee’s findings. However, a deposit with a

pronounced (220)-(211) combination showed almost no whiskers, which according to Lee and Lee, should have grown whiskers from the less dominant crystal plane. In a similar manner as Lee and Lee, we looked for a relationship between the crystal planes and their corresponding main texture planes have very similar values. The interplanar angle Φ is the angle between the normals of two crystal planes. For the (101)-(103) combination, this angle is 13.0° , for (211)-(321) 13.7° , and for (220)-(420) 18.7° . This is very different from the angle of the low-whisker combination (220)-(211) which is 42.8° .

Stereographic Projection

A convenient tool to visualise Φ is the stereographic projection, where the *normals* of the planes are projected onto a globe that wraps around the elementary cell. (See Figure 1.)

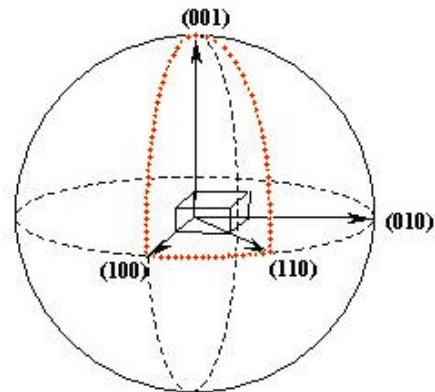


Figure 1 – Stereographic Projection of the Elementary Cell of b-Tin

This is slightly different from the standard stereographic projection, where the *crystal orientations* are projected onto the globe. This technique differentiates between cubic and tetragonal systems and therefore provides higher accuracy for tin, which is a tetragonal system.

The resulting triangle (dotted lines in Figure 1 with (001), (100) and (110) as corners) can now be used to map the crystal planes of β -tin (Figure 2).

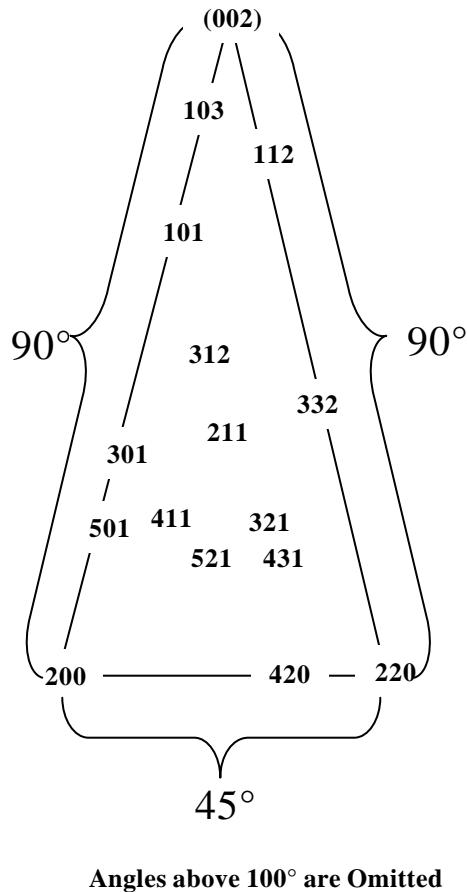


Figure 2 – β -Tin Crystal Plane ‘Map’, Crystallographic Extinguished Planes (with the exception of 002) and Plane s Showing 2 θ

The positions of the planes in the triangle correspond to the spatial position of the planes in the elementary cell. Thus, the distances between the crystal planes correspond directly to Φ .

Crystal Planes in Electrodeposits

A look at typical XRD patterns of electrodeposits reveal that the observed crystal planes cover a relatively small portion of the possible crystal planes. However, it has been observed that the predominant crystal plane of a deposit is surrounded by closely related crystal planes. Interestingly, it was also observed that common electroplated tin deposits with a relatively narrow range of closely related crystal planes are most prone to whisker growth. In contrast, deposits with a wider distribution, or deposits with a *very* narrow crystal plane distribution have a significantly lower risk to grow tin whiskers. From this, a range for Φ between 5 and 22° has been determined, in

which tin deposits show a noticeably higher tendency towards whisker growth. (See Figure 3.)

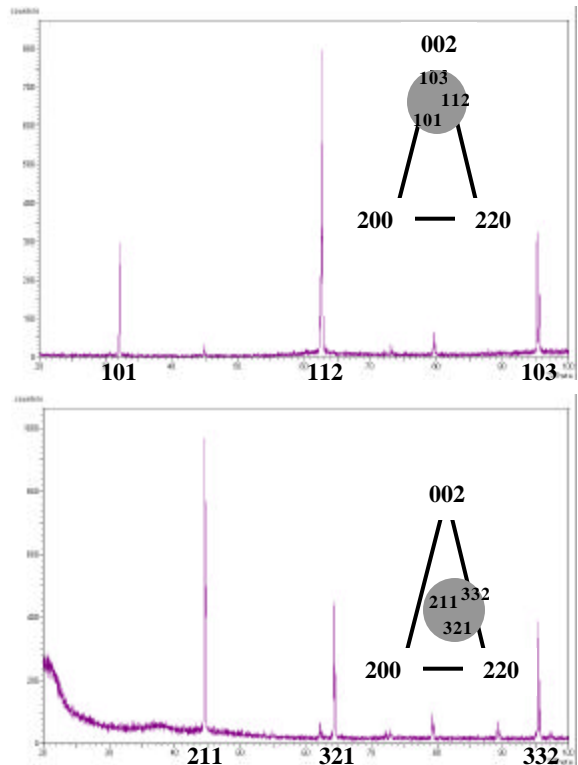


Figure 3 – XRD-Mapping of Electrodeposits

Limitations of the Q-2 θ -Scan: Equivalent Planes

The screening of several XRD patterns in regard to the 5 to 22° range and its relevance for whisker growth probability revealed that a number of exceptions to the theory exist. These exceptions are mainly due to the existence of equivalent crystal planes, which have been neglected so far. Figure 1 shows only part of one hemisphere of the globe that has been selected to describe the β -tin system. All the other positions on the globe can easily be constructed by geometrical operations from the positions in the selected triangle of Figure 2. They have the same d-line spacing resulting in the same 2θ angle and are called equivalent planes (Figure 4).

Due to the possibility of clearly defined geometric transformations, the planes of a crystal system are usually sufficiently described by (hkl). However, for the calculation of Φ , all equivalent planes have to be taken into account. For a tetragonal system such as tin, these planes are (hkl), (-hkl), (h-kl), (-h-kl), (khl), (-khl), (k-hl), (-k-hl), (hk-l), (-hk-l), (h-k-l), (-h-k-l), (kh-l), (-kh-l), (k-h-l), (-k-h-l). Thus, the angle between two crystal planes (hkl)₁ and (hkl)₂ is only a fraction of the many possible angles between all equivalent planes of a crystal plane pair.

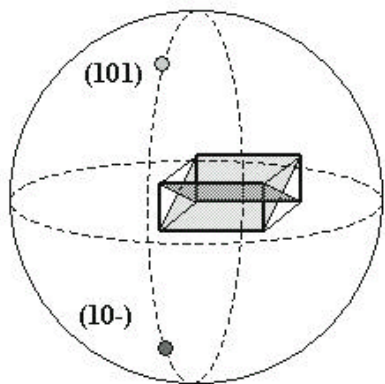


Figure 4 – An Equivalent Crystal Plane of (101). For clarity only two planes are depicted.

The fact that an observed XRD peak not only corresponds to one crystal plane but to a family of equivalent planes has significant consequences: i) A crystal plane pair that has been considered as critical, i.e. that shows Φ between about 5 and 22°, is maybe not so very critical because many non-critical interplanar angles between equivalent planes exist. ii) The opposite is of course also true - non-critical combinations might be more critical than initially estimated. iii) The existence of equivalent planes allows the formation of interplanar angles between planes of the same family.

Crystallography of b-tin

A careful analysis of all possible interplanar angles Φ shows that not only the range between about 5 and 22° is critical for whisker growth, but that additional ranges of roughly 80 to 90° and from 158 to 175° have an impact on whisker growth. The tetragonal symmetry of tin explains the influence of the 158 to 175°, which simply corresponds to 180°-(5 to 22°). A similar situation would occur at 90°-(5 to 22°), if tin were a cubic system.

Since this is not the case, the crystallographic system of tin was examined in regard to its resemblance to a cubic system. It was indeed found that β -tin could be interpreted as a distorted primitive cubic crystal system. Thus, if two tin cells are stacked, almost a cube is formed having side lengths of 5.83 Å and 6.36 Å, respectively as shown in Figure 5.

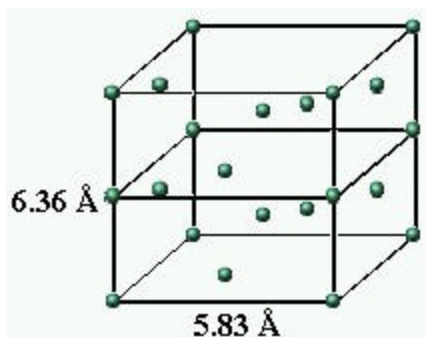


Figure 5 – Two Tin Cells, Almost a Cube.

This approach explains to a certain extent that interplanar angles close to 90° have a similar effect like Φ -values between about 5 and 22°. The distortion from the cubic cell is responsible for the narrowing of the critical range. The final critical ranges are shown graphically in Figure 6.

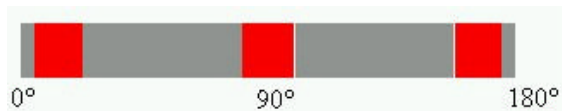


Figure 6 – Critical Ranges of Angle F.

Whisker Growth Probability Calculation

Because of the existence of equivalent crystal planes that cannot be observed by XRD in a Θ -2 Θ scan, the observed crystal plane pairs cannot be used alone to determine a deposits propensity to whisker. A factor, F_{ca} , is calculated by taking the fraction of critical angles (i.e., angles between 5 and 22°) of all crystal plane combinations, including equivalent planes, in an observed crystal plane pair. A method to estimate the whisker growth probability of a given tin deposit is proposed by the following equation:

$$N_{wp} = [\sum \{ (Irel_{K\alpha 1, h_1 k_1 l_1}) * (Irel_{K\alpha 1, h_2 k_2 l_2}) * F_{ca} \}_x] * 100$$

N_{wp} : Whisker probability number

$Irel_{K\alpha 1, h_1 k_1 l_1}$: Relative intensity obtained from the diffraction of $K_{\alpha 1}$ radiation on plane $h_1 k_1 l_1$ expressed as a fraction of 1.

$Irel_{K\alpha 1, h_2 k_2 l_2}$: Relative intensity obtained from the diffraction of $K_{\alpha 1}$ radiation on plane $h_2 k_2 l_2$ expressed as a fraction of 1.

x: To obtain the sum (Σ), all crystal pair combinations, including equivalent crystal planes, must be calculated. This is represented by x.

F_{ca} : Fraction of critical angles

The deposits that correspond to the patterns of (A) and (B) in Figure 7 have N_{wp} 's of 8 and 20.5, respectively. Actually, a 10 μ m thick tin deposit (B) showed many whiskers after very short storage times, whereas a 10 μ m thick tin deposit of (A) was whisker-free after 6 months. Both deposits were plated over C 194 and had been stored under the same conditions. Numerous observations have shown that an N_{wp} of about 10 corresponds to the limit that decides whether a 10 μ m deposit will exhibit whiskers or not. It is, however, important to recognize that N_{wp} is a relative term and therefore most useful for comparing systems of similar grain size, same deposit thickness, same substrate, same pre-treatment process and other similar factors known to influence whisker growth.

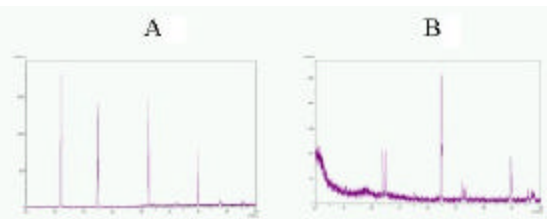


Figure 7 – XRD Patterns of a Low (A) and a High (B) Whisker Risk Deposit

Grain Boundary Architecture

Interestingly, the 5 to 22° range corresponds approximately to the range of small angle grain boundaries. A grain boundary may be defined as the interfacial transition region between two perfect crystals, which are in contact to each other but are differing in crystallographic orientation.³ This definition and the above reported observation that whisker growth is somehow related to interplanar angles (which are the result of different crystallographic orientations) implies that the architecture of the grain boundaries is of significant importance. Grain boundaries may also be defined as an array of dislocations which absorb and emit vacancies. The rate of this absorption-emission mechanism will largely depend on the degree of mismatch in the grain boundary, and therefore again from the different crystallographic orientation of two neighbouring grains.

Thus, the larger the difference in crystallographic orientation (i.e., the larger the interplanar angle between the crystal planes of two adjacent grains), the more absorption and emission of vacancies will be observed. In brief, the diffusion in large angle grain boundaries is fast, and the diffusion in small angle grain boundaries is slow.

Creep Mechanisms⁴

It is widely accepted that whisker growth is a stress relief phenomenon. An important characteristic of tin is its high homologous temperature of about 0.6 at room temperature (T/T_m , where T_m is the melting temperature). Because of this high homologous temperature, Coble creep is observed even at relatively low applied stress values.^{5,6} Usually, Coble creep is described as grain boundary diffusion. In its mathematical form, it is expressed as, $\dot{\epsilon} = 45\sigma\Omega\delta D_{GB} / d^3kT$, where σ is a shear stress, Ω is the atomic volume, δ is the width of the grain boundary, D_{GB} is the grain boundary diffusion coefficient, and d is the grain diameter. The $1/d^3$ dependency favours Coble creep at small grain sizes. This, and the strong dependency of whisker growth on grain size and deposit thickness imply that grain boundary diffusion contributes substantially to whisker growth.

In 1976, a two-stage model for whisker growth was proposed by Lindborg.⁷ The first stage of the model, diffusion, is described as whisker growth rate, $h' = 2D_{GB}\delta\sigma\Omega / R_w dkT$, (R_w is the whisker radius, d corresponds to the average grain diameter). The second

stage of Lindborg's model corresponds to dislocation glide as a result of an increasing shear stress around the whisker. According to Lindborg, the sliding stage is governed by this stress and an opposing stress from the deposit due to a dislocation 'forest' inside the grains. The opposing stress caused by the dislocation forest acts as a barrier which must be overcome before gliding can occur. Thus, the larger the spacing between these dislocations is, the lower is the internal (opposing) stress, and the easier it is for whiskers to grow. The texture effect is tentatively explained by different implications of the shear stress on the slip planes of grains having different crystallographic orientations.

Modification to The Two-Stage Model

The considerations above imply that more obstacles in the deposit are beneficial to decrease whisker growth. This, however, is in contradiction to the observation that small-angle grain boundary dominated deposits are substantially more prone to whisker growth than large-angle grain boundary deposits. Yet, Lindborg localised the root for the opposing stress mainly *inside* the grains and his treatment relates to zinc deposits and not necessarily to tin.

This is where the present investigation becomes significant. As already stated, at room temperature the homologous temperature of tin is high and Coble creep (i.e., grain boundary diffusion) is active at low stress values. At high stress values, gliding processes begin to occur. For the following considerations it is assumed that dislocations occur only in the grain boundaries and not inside the grains themselves. In the case of whisker growth of tin plated copper substrates, the initial source of stress is related, at least in part, to the rate and the amount of newly formed Cu_6Sn_5 intermetallic compound. At this first stage, when only little Cu_6Sn_5 has formed and therefore little stress introduced to the system, Coble creep of tin will be the preferred diffusion mechanism. This grain boundary diffusion of tin will continue until such time as no more vacancies are available to fill. The temporary inability for tin to self-diffuse causes a spontaneous and localized build-up in stress. It is at this point that Coble creep is replaced by dislocation glide as the dominant method to accommodate the persistent movement of tin, and whisker growth begins.

High concentrations of intermetallic compound will introduce higher levels of stress to the system. It is logical to imagine then that in these cases of higher stress it will take less time for dislocation glide to initiate, and whisker growth will occur more rapidly.

Conclusion

The degree of grain boundary diffusion will depend on the grain boundary dimension and the grain size. The combination of small grains and large grain boundaries leads to high creep values, whereas large grains and small grain boundaries result in low creep values. As stated

previously, a grain boundary is the zone between where two crystal planes of different orientation meet, creating an interplanar angle. The lower this angle, the narrower the grain boundary. By definition, grain boundaries contain a high concentration of vacancies and imperfections. It follows then that narrower grain boundaries will contain fewer vacancies and diffusion pathways, and the tin will therefore fill these available vacancies more quickly.

As discussed above, the final stages of vacancy filling will be accompanied by an increase in stress and a shift to the stress-induced gliding mechanism associated with whisker growth. It is therefore seen that where interplanar angles are high, i.e., grain boundaries are wide and vacancies numerous, that the time for stress to build to the point of initiating dislocation glide will be delayed, perhaps indefinitely. Grain boundary dimensions corresponding to interplanar angles above 22° are believed to allow for sufficient movement of tin without stress build-up to the point where whisker growth would be initiated.

Discussion

In general, the observed influence of crystal planes on whisker growth and the proposed whisker growth mechanism imply that tin deposits which show a fast tin-in-tin diffusion (self diffusion) are less prone to whisker growth than tin deposits with a slow self-diffusion. Interestingly, the only report in the literature (which the authors are aware of) that combines experimental diffusion data directly with whisker growth shows that slow self-diffusion favours whisker growth.⁸ It is also worthy to note that already in the 1950's, Ellis et. al. reported the possibility that impurities inside the deposit could block diffusion and thereby serve as seeds where whisker growth starts.^{9,10} If the concept of impurities is made analogous with the narrowing of grain boundaries, it is interesting how well the presently proposed whisker growth mechanism is captured by this description.

With respect to Lindborg's mechanism, the present mechanism differs primarily in that Lindborg describes reducing obstacles inside the grain until gliding becomes possible, whereas the present mechanism assumes an unconstrained grain boundary that gets tighter until the conditions for gliding are fulfilled. It is a start from two different viewpoints, but ends with a similar result.

References

1. Lee, B.-Z.; Lee, D.N., *Acta Mater.*, 1998, **46**, 3701.
2. Xu, C.; Zhang, Y.; Fan, C.; Chiu, P., Abys, J.A., *Plating & Surface Finishing*, 2000, Sept., 88.
3. Kaur, I.; Mishin, Y.; Gust, W., in *Fundamentals of Grain and Interphase Boundary Diffusion*, 3rd ed., 1995, Wiley.
4. Thorsen, P.A., 1998, PhD Thesis, Risø-R-1047, Risø Nat. Lab.
5. Coble, R.L., *J. Appl. Phys.*, 1963, 34, 1679.
6. Ashby, M.F., *Acta Metal.*, 1972, 20, 887.
7. Lindborg, U., *Acta Metal.*, 1976, 24, 181.
8. Kehrler, H.-P.; Kadereit, H.G., *Appl. Phys. Lett.*, H.G., 1970, 16, 411.
9. Ellis, W.C.; Gibbons, D.F.; Treuting, R.G., in *Growth and Perfection of Crystals*, 1958, Wiley.
10. Politycki, A.; Kehrler, H.-P., *Z. Metallkde.*, 1968, 59, 309.